Yield stress in magnetorheological and electrorheological fluids: A comparison between microscopic and macroscopic structural models

Yield stress in magnetorheological and electrorheological fluids: A comparison between microscopic and macroscopic structural models

G. Bossis,[a] E. Lemaire, and O. Volkova

Laboratoire de Physique de la Matière Condensée, Parc Valrose, 06108 Nice Cedex 02, France

H. Clercx

Department of Physics, Eindhoven University of Technology, P.O. Box 513, 5600 MB Eindhoven, the Netherlands

(Received 21 October 1996; final revision received 27 December 1996)

Synopsis

The yield stress of a magnetorheological suspension is calculated from two different approaches. The first one is based on a mesoscopic description of the structure taking only into account the shape anisotropy of the strained aggregates. The second one is based on a microscopic approach where the interparticle forces, due to the application of the field, are calculated numerically by taking into account the magnetostatics between the particles inside the aggregates. We show that the macroscopic description well applies to suspensions of nonmagnetic particles in a ferrofluid and that a layered structure, consisting of parallel slabs of magnetizable materials should have a yield stress much higher than a structure made of cylindrical aggregates. On the other hand the microscopic approach is appropriated for the description of suspensions of particles of high permeability. In this case, the yield stress is mainly determined by the rupture between pairs of particles and, consequently, it strongly increases with the angle between the line of centers of the pair undergoing the rupture and the field. © *1997 The Society of Rheology.* [S0148-6055(97)00203-4]

I. INTRODUCTION

Magnetorheological suspensions have received less attention than electrorheological suspensions mainly because the weight and the space required by the coils to produce the magnetic field was thought to be a severe restriction for practical applications. Furthermore the response time of the fluid is limited by the rising time $\tau = L/R$ (with L the inductance and R the resistance of the coils) of the magnetic field which, in practice, is of order 10^{-1} to 10^{-2} s. Nevertheless, just comparing the magnetostatic energy density $\mu_0 H^2{}_0$ for $H_0 = 3000$ Oe and the electrostatic energy density $\epsilon_0 E^2{}_0$ for a field $E_0 = 3$ kV/mm (close to the breakdown field) it appears that the former is larger by an order of magnitude. This is the first reason why yield stresses obtained with magnetorheological (MR) fluids are much larger than those obtained with electrorheological (ER) fluids. Yield stresses close to 100 kPa are obtained with magnetic suspensions containing a powder of carbonyl iron (Weiss *et al.*, 1994), whereas 15 kPa seems to be

[a]Corresponding author.

the maximum yield stress ever obtained with an ER fluid (Haveka, 1994). Furthermore these ER fluids are difficult to use commercially due to a too high power consumption. Of course this argument based on stored energy in vacuum should be modified to account for the storage capacity of the medium which is characterized by its dielectric constant ϵ for ER suspensions or by its magnetic permeability μ for MR suspensions. For instance the electrostatic energy density will be: $W = 0.5\epsilon_0\epsilon E^2$, where ϵ is the relative permittivity of the suspension and E an average electric field. When the suspension is strained by a quantity γ, the energy will generally decrease due to forced nonalignment of the aggregates with the external applied field. This will give rise to a restoring stress

$$\tau = -\frac{\partial W}{\partial \gamma} = \frac{\epsilon_0 E^2}{2}\frac{\partial \epsilon}{\partial \gamma}. \tag{1}$$

The observation of this fundamental equation already tells us that it is change of permittivity with the strain which gives the magnitude of the yield stress. The energy stored in the suspension can change because some macroscopic aggregates are being deformed or rotated in the field but also because of small motions at interparticle distance scale. Obviously these two mechanisms are always present in MR or ER fluids but we are going to study the two extreme situations and we shall show that we can find fluids which follow quite well one or the other model. The first part of this article will be devoted to a macroscopic model which generalizes the one recently proposed by Rosensweig (1995). The second part is based on a microscopic derivation which uses a multipolar development of the magnetic (or electric) field in order to determine the permeability (or the permittivity). This derivation takes into account the microstructure and allows one to test the validity of the macroscopic model in different situations.

II. MACROSCOPIC APPROACH

In this first approach to obtain the yield stress in ER or MR fluids we consider macroscopic structures which are only characterized by their shape (stripes, cylinders, ellipsoids...) and by their internal volume fraction. We ignore any internal structure inside the aggregates, so the change of energy when the suspension is strained only comes from shape effects and could be roughly approximated by the change of energy of a solid rotating in the field. In the following we shall use the notations corresponding to MR fluids but all results apply quite well for ER fluids when the relevant magnetic parameters are replaced by their electrostatic counterparts. Actually it should even apply better to the case of ER fluids where the metallic electrodes bring charges which fix the average Maxwell field: $E = V/d$ everywhere in the sample, whereas the modulation of the magnetization imposed by the intersection of the mesoscopic structure with the surface of the sample gives rise to a modulation of the average field which is neglected in this approach.

The energy of a body of permeability μ_s introduced in a medium of permeability μ_f in the presence of a field H_0 is given by (Landau and Lifschitz):

$$W = -\frac{1}{2}\int_{v_s} (\mu_s - \mu_f)\mathbf{H}.\mathbf{H}_0 dV_a\,, \tag{2}$$

where $\mathbf{H}$ is the new field in the presence of the aggregate and V_a the volume of the aggregate. If we call $\mathbf{m}$ the increment of the magnetic moment obtained by replacing the initial medium of permeability μ_f by the one of permeability μ_s Eq. (2) becomes:

$$W = -\frac{1}{2}\mathbf{m}.\mathbf{H}_0\,. \tag{3}$$

The shear force per unit surface τ is given by the derivative of the energy:

$$\tau = \frac{F_y}{S} = -\frac{1}{S}\frac{\partial W}{\partial y} = -\frac{1}{V}\frac{\partial W}{\partial \gamma},$$

where $\gamma = y/d$ is the strain and V the volume of the sample. Then taking the energy from (3) we obtain

$$\tau = \frac{1}{2V} H_0 \frac{\partial m_z}{\partial \gamma}. \tag{4}$$

In Eq. (4) m_z is the component of the magnetic moment of the sample along the direction of the external field

A. Ellipsoidal aggregates

Rheological models are usually based on ellipsoidal aggregates (Shulman *et al.*, 1986, Halsey *et al.*, 1992) because the magnetization is constant inside an ellipsoid placed in a constant external field. The components of the magnetic moment in the frame (Ox',y',z') of an ellipsoidal aggregate with a main axis of length d and a small axis of length b are, respectively, (Landau and Lifschitz):

$$m_a^{\|} = \alpha_{\|} H_0 \cos\theta \quad \text{and} \quad m_a^{\perp} = -\alpha_{\perp} H_0 \sin\theta,$$

with

$$\alpha_{\|} = \frac{(\mu_s - \mu_f)V_a}{1+\mu_s^* n_{\|}}$$

and

$$\alpha_{\perp} = \frac{(\mu_s - \mu_f)V_a}{1+\mu_s^* n_{\perp}}.$$

In this formula θ represents the angle between the main axis of the aggregate (along Oz') and the field H_0 aligned along Oz; the quantities $\alpha_{\|}$ and $\alpha_{\perp}$ are the magnetic polarizabilities along the main axes of the ellipsoid and $n_{\|}$ and $n_{\perp}$ are the demagnetization factors of an ellipsoid given by:

$$n_{\|} = \frac{1-e^2}{2e^3}\left[\log\left(\frac{1+e}{1-e}\right) - 2e\right],$$

with

$$e = \sqrt{1-(b^2/d^2)} \quad \text{and} \quad n_{\perp} = (1-n_{\|})/2.$$

Finally, $\mu_s^* = (\mu_s/\mu_f) - 1$ represents the relative difference of permeability between the aggregate and the suspending medium and V_a the volume of the ellipsoidal aggregate. In order to obtain the energy we need the component of the magnetic dipole of the aggregate along the direction z of the field:

$$m_a^z = (\mu_s - \mu_f)H_0\left(\frac{\cos^2\theta}{1+\mu_s^* n_{\|}} + \frac{\sin^2\theta}{1+\mu_s^* n_{\perp}}\right)V_a. \tag{5}$$

If we assume that the aggregates do not interact with each other, the total magnetic moment of the sample will be $m_z = N_a m_a^z$, with N_a the number of ellipsoidal aggregates. Introducing the internal volume fraction Φ_a inside the aggregates and the initial average volume fraction Φ we shall have, using (4):

$$\tau = \frac{1}{2}\frac{\Phi}{\Phi_a} H_0 \frac{\partial(m_a^z/V_a)}{\partial\gamma}. \tag{6}$$

The strain is related to the angle θ by $\gamma = \mathrm{tg}\theta$. So replacing m_a^z/V_a by (5) yields:

$$\frac{\tau}{\mu_f H_0^2} = \frac{1}{2}\frac{\Phi}{\Phi_a}\mu_s^* \frac{\partial}{\partial\gamma}\left(\frac{1}{(1+\gamma^2)(1+\mu_s^* n_{\|})} + \frac{\gamma^2}{(1+\gamma^2)(1+\mu_s^* n_{\perp})}\right). \tag{7}$$

This expression does not take into account the striction of the aggregate during the strain. This can be done by noting that for an angle θ the length of the major axis becomes $d' = d/\cos\theta$, with $\cos\theta = 1/(1+\gamma^2)^{1/2}$. The invariance of the volume involves $b' = b(\cos\theta)^{1/2}$ and the demagnetization factor which is a function of the ratio b'/d' will become a function of $b(\cos\theta)^{3/2}/d$.

The stress versus the strain with and without striction is shown in Fig. 1 for a ratio $b/d = 0.1$, an average volume fraction $\Phi = 0.3$, and an internal volume fraction $\Phi_a = 0.64$; this value is motivated by the assumption that the ellipsoids are aggregates of randomly closed spherical aggregates. We see that the effect of striction can be neglected.

Actually this model is only valid in the limit of low volume fractions. For higher volume fractions it is more appropriated to consider a mean field theory where each ellipsoid is immersed in the average medium of volume fraction Φ and of permeability $\mu(\Phi)$. In this case we can take, instead of the external field H_0 the field $H = H_0/\mu(\Phi)$. The same relation as (7) will hold but the field which normalizes the stress is the average field H instead of H_0 and in the relative permeability μ_s^* we have to replace μ_f by the average permeability of the suspension:

$$\mu_m^* = \frac{\mu_s(\Phi_a)}{\mu(\Phi)} - 1.$$

Keeping the same normalization as in (7) for the stress we have:

$$\frac{\tau}{\mu_F H^2} = \frac{1}{2}\frac{\Phi}{\Phi_a}\frac{\mu(\Phi)}{\mu_f}\mu_m^* \frac{\partial}{\partial\gamma}\left(\frac{1}{(1+\gamma^2)(1+\mu_m^* n_{\|})} + \frac{\gamma^2}{(1+\gamma^2)(1+\mu_m^* n_{\perp})}\right). \tag{8}$$

The relation between the permeability of the suspension and the volume fraction is unknown, but we have shown (Volkova *et al.*, 1996) that a mean field theory, such as the Maxwell-Garnet (1904) theory, well represents this dependence at least for suspensions of non magnetic particles in a ferrofluid. In this case we have:

$$\frac{\mu(\Phi)}{\mu_f} = \frac{1+2\beta\Phi}{1-\beta\Phi}$$

where

$$\beta = \frac{\alpha-1}{\alpha+2} \text{ with } \quad \alpha = \frac{\mu_p}{\mu_f}, \tag{9}$$

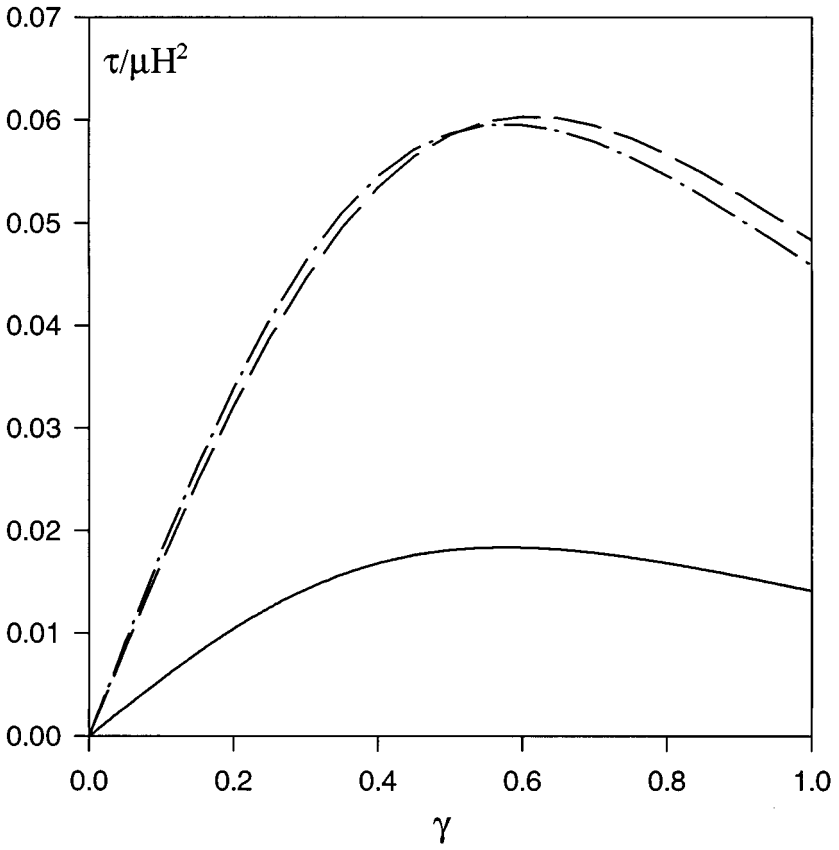

FIG. 1. Normalized stress vs strain for ellipsoidal aggregates of internal volume fraction $\Phi_a = 0.64$. The average volume fraction is $\Phi = 0.3$ and $\alpha = \mu_p/\mu_f = 0$. — - — - — Eq. (7) with aspect ratio $b/a = 0.1$; striction not included. — — — Eq. (7) with aspect ratio b/a:0.1; striction included. —— Eq. (8): with aspect ratio $b/a = 0.1$. H is now the average field inside the sample.

where μ_p is the particles permeability. For suspensions with particles of high permeability in a nonmagnetic fluid we have $\beta \cong 1$ and for suspensions of nonmagnetic particles, in a high permeability ferrofluid we have $\beta \cong -0.5$. Of course the relation (9) normally applies to a random medium but we shall assume that the permeability does not change drastically when the suspension is structured by the magnetic field.

The relation (9) can also be used to obtain the internal permeability of the aggregate: $\mu_s(\Phi_a)$. Then with the help of Eqs. (7) and (9) or (8) and (9) we can predict the stress-strain relation. In Fig. 1 the lower curve (solid line) is obtained from Eq. (8) for an average volume fraction $\Phi = 0.3$ and $\beta = -0.5$. We see that, compared to the upper curves where each aggregate is considered alone in the external field, the mean field approach gives a much lower value of the stresses. This is quite understandable since at high volume fraction the fields H and H_0 are quite different. If we take $H = H_0/\mu(\Phi)$ with $\mu(\Phi) = 0.609$ in the l.h.s. of Eq. (8), the difference persists but is much lower.

Another approach consists of considering a network of aggregates and calculating the change of energy when this network is strained. This approach has been used recently

(Rosensweig, 1995) for a layered structure. Actually, depending on the volume fraction, we can observe structures formed of isolated cylinders or labyrinthine structures which transform into well aligned stripes in the presence of a flow (Bossis *et al.*, 1994, Grasselli *et al.*, 1994, Liu *et al.*, 1994).

B. Stripes and cylinders

We have generalized the model presented by Rosensweig who has only considered the stress coming from the torque and we have also extended it to the case of a lattice of cylinders. This model has been presented elsewhere (Lemaire *et al.*, 1996) and, for completeness, the main steps are summarized in Appendix A.
The analytic result for the normalized stress is:

$$\frac{\tau}{\mu_f H^2} = -\frac{1}{2}(\mu_s^*)^2 \frac{2\gamma}{(1+\gamma^2)^2} \frac{\Phi_s(1-\Phi_s)}{C_s+\mu_s^*(1-\Phi_s)}, \quad \text{with } \Phi_s = \frac{\Phi}{\Phi_a} \tag{10}$$

and $C_s = 1$ for stripes or $C_s = 2$ for cylinders. The minus sign expresses the fact that it is a restoring stress; in the following we shall consider the absolute value. The maximum of the stress relatively to the strain is obtained for $\partial\tau/\delta\gamma = 0$ which gives $\gamma_c = \sqrt{3}/3$.

In this model the demagnetization is taken into account only in average since it is the average field H and not the external field H_0 which normalizes the stress. The demagnetization factor is known for periodic stripes with zero inclination relatively to the field (Cebers, 1995). A calculation could likely be done taking into account the inclination of the aggregates, if we assume that the magnetization is constant throughout the stripe—which in turn implies that the tangential field varies from place to place. It is not sure that it is a better approximation and we shall see in Sec. III that the agreement is already good without considering this dependence.

In Fig. 2 he have plotted $\tau/\mu H^2$ versus the strain for the three cases we have seen. We have taken an average volume fraction $\Phi = 30\%$ and $\Phi_a = 64\%$ for the internal volume fraction of the aggregates. We have used $\alpha = \mu_p/\mu_f = 0$ which would correspond to the case of magnetic holes ($\mu_p = 1$) in a ferrofluid of infinite permeability. In this case the internal permeability given by (9) for $\Phi = \Phi_a = 64\%$ and $\beta = -0.5$ is $\mu_s/\mu_f = 0.273$. The solid curve and the dash-dotted line correspond to the ellipsoidal aggregates [Eq. (8)] and to cylindrical aggregates, respectively. They are not very different which is quite expected due to their similar shape. On the other hand the upper curve, obtained for a slab structure, predicts a yield stress approximately three times higher than for cylindrical or ellipsoidal aggregates.

III. MICROSCOPIC DERIVATION OF THE YIELD STRESS

In a microscopic derivation of the yield stress we have to know the precise position of each particle in the suspension and also the way they will move when the suspension is strained. This calculation can be done either by a finite element method (Davis, 1992) or by a multipolar expansion (Chen *et al.*, 1991, Clercx and Bossis 1993, 1995) This last method, although limited to linear media, is more powerful. For any configuration of the particles the total dipole moment per unit volume can be calculated by solving a set of linear equations:

$$\beta a^3 \mathbf{H} = \mathbf{C}\cdot\mathbf{m}. \tag{11}$$

In Eq. (11) a is the radius of the particles and β is defined in Eq. (9). If we use a periodic lattice with N particles located in a unit cell, then $\mathbf{H}$ is the average field inside

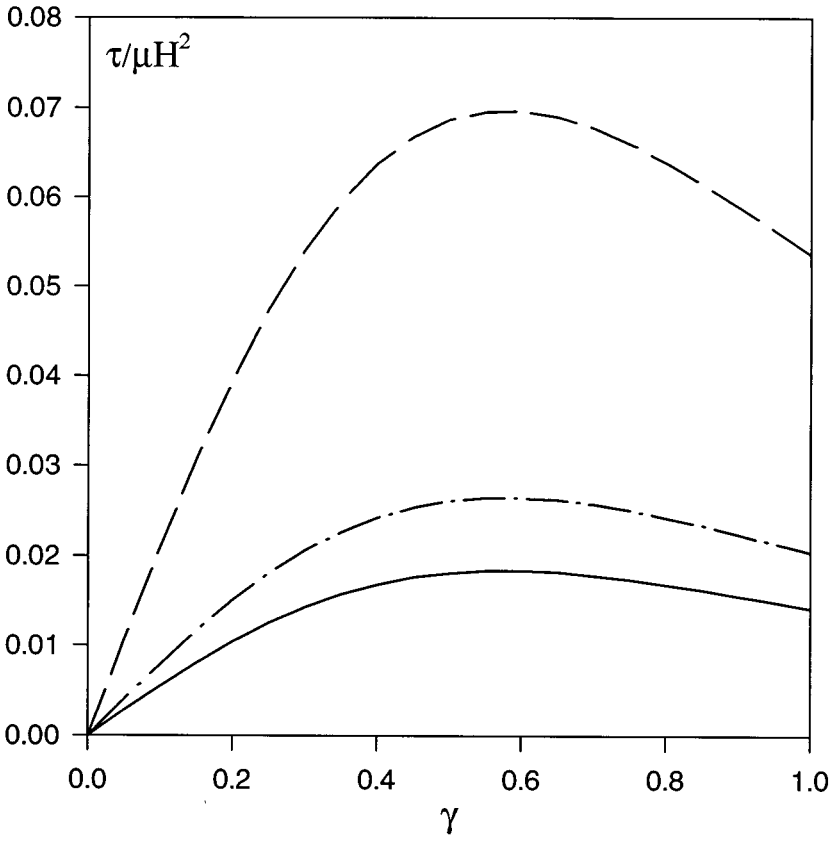

FIG. 2. Normalized stress versus strain for different models of aggregates of internal volume fraction $\Phi_a = 0.64$. The average volume fraction is $\Phi = 0.3$ and $\alpha = 0$. —— Eq. (8): ellipsoidal aggregates aspect ratio 0.1, — - — - Cylindrical aggregates: Eq. (10) with $C_s = 2$, — — — Stripes: Eq. (15) with $C_s = 1$.

the unit cell (here a $3N$ vector), **C** is a $3N \times 3N$ matrix which depends on the relative positions of the particles inside the unit cell, and **m** the $3N$ vector defining the dipolar moment of each particle. For particles of high permeability or permittivity (in practice $\alpha = \mu_p/\mu_f > 5$), the dipolar approximation becomes very poor and we need to use a multipolar development of the potential of the magnetic (or electric field). In this case the matrix **C** takes into account the short range multipolar interactions; it is obtained by a partial inversion of the set of equations containing the multipoles of order larger than one (Clerex and Bossis, 1993). Once the dipole moment of a unit cell for a given strain, denoted by $\mathbf{m}(\gamma)$, is known, the stress is obtained from the derivative of the energy, cf. Eq. (4), where H_0 must be replaced by H, the average field. In a previous investigation we have used this approach to obtain the yield stresses of different lattices relatively to the volume fraction and to α(Clercx and Bossis, 1995). We are going to use the same method to test the applicability of the macroscopic model derived in the first section. This test has been carried out for structures of cylinders and stripes, both for low and high values of α. For the low values we have taken $\alpha = 0$ and $\alpha = 0.135$ This last value corresponds to a suspension of nonmagnetic spheres in a ferrofluid. For the high values

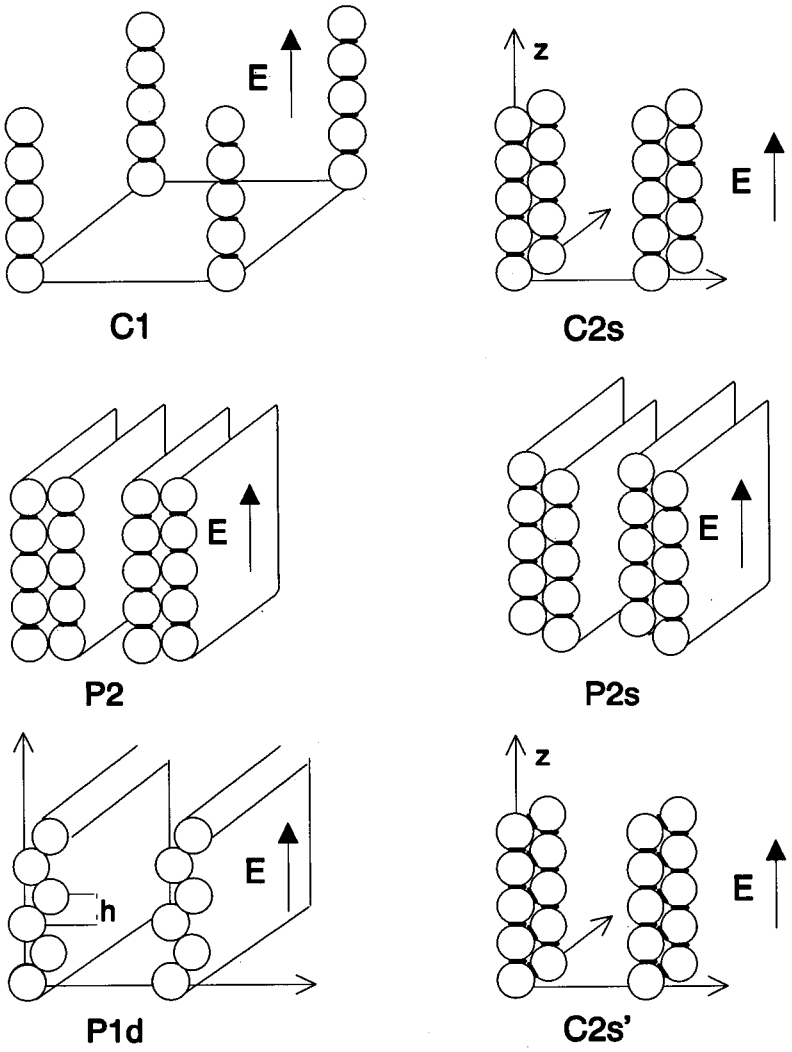

FIG. 3. Different structures studied. The corresponding yield stresses are reported in Table I. The thick neck between the spheres indicate the points of rupture when the begin to shear. In P1d these points are not shown since the rupture will happen after the chain is completely extended for $\gamma_c = \sqrt{(16a^2/h^2)-1}$. Note the difference of rupture points between C2S and C2S′; in this last case the altitude of each particle will remain constant contrarily to C2S.

we have taken $\alpha = 10$, $\alpha = 38$, and $\alpha = 50$. These values are representative of the permeability for steel bearing balls at intermediate values of the magnetic field.

A. Comparison with the macroscopic approach for $\alpha<1$

We have first considered a simple cubic lattice of chains (cf. Cl Fig. 3) with particles which move affinely in a simple shear flow: $V_y = \dot{\gamma}z$. Each chain is assimilated to a cylinder. Then the results obtained by the microscopic approach are compared to the prediction of the macroscopic theory for cylinders. We have carried out this comparison for two values of $\alpha = \mu_p/\mu_f$, namely $\alpha = 0$ and $\alpha = 0.135$. We have taken for the

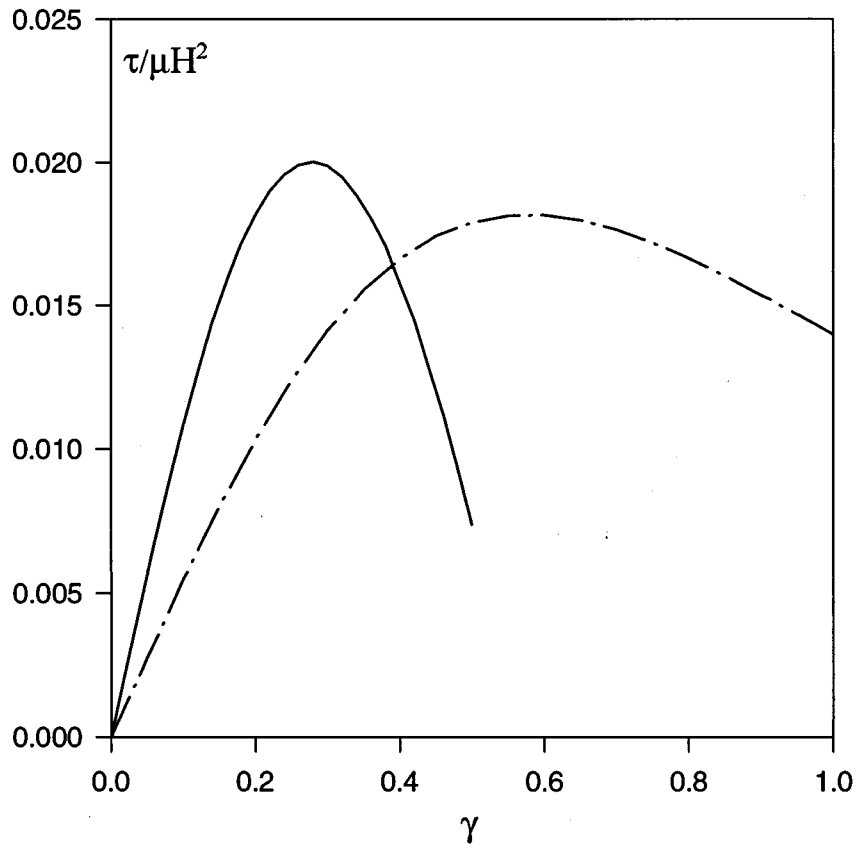

FIG. 4. Comparison between microscopic and continuum models for cylinders with $\alpha = 0.135$ and an average volume fraction $\Phi = 0.4$ —— microscopic model: cubic network of chains, — - — - continuum model for cylinders with $\Phi_a = 2/3$.

apparent volume fraction inside the aggregates appearing in Eq. (10) the fraction corresponding to a chain of spheres in a cylinder of same radius, $\Phi_a = 2/3$. The stress versus strain curves are shown in Fig. 4 for $\alpha = 0.135$ and $\Phi = 0.4$. The solid curve is the result of the numerical calculation and the dash-dotted curve the prediction of Eq. (10). It appears that the critical strain γ_c corresponding to the maximum of the curve is too large in the macroscopic model ($\sqrt{3}/3$ instead of 0.3); this is likely due to the fact that in the microscopic model the distance between the centers of the particles increases during the strain which makes the force fall off for smaller strains than in the macroscopic model where the interparticle distance does not appear. Nevertheless, the agreement for the maximum stress is remarkably good taking into account that we have no free parameter. This is not accidental as we can see in Fig. 5 where we have compared the yield stress—which is the maximum of the stress-strain curve—predicted by the two models for $\alpha = 0$ and $\alpha = 0.135$. It appears that for these two values of α the agreement between the two models is quite good: in the worst case for $\alpha = 0.135$ and $\Phi = 0.5$ the disagreement is less than 20%. It is interesting to note that we have an optimum volume fraction for the yield stress, which is around 30%.

A similar comparison between macroscopic and microscopic models is presented in

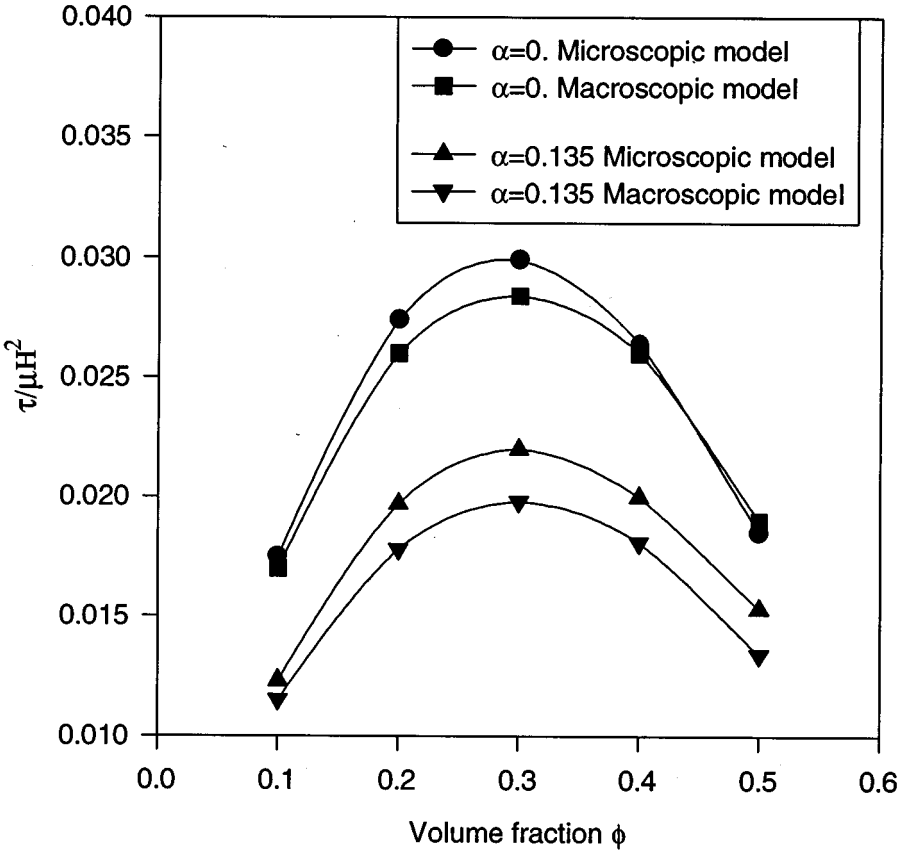

FIG. 5. Normalized yield stress versus volume fraction. Comparison between microscopic and continuum models for a structure made of cylindrical aggregates.

Fig. 6 for a layered structure. In the microscopic model the stripes are formed by two (cf. P2 Fig. 3) or four planes of particles having an internal volume fraction $\Phi_a = \pi/6$ corresponding to a simple cubic packing. The distance between the stripes is fixed by the knowledge of the average volume fraction. The solid curve in Fig. 6 represents the result of the numerical simulation for $\alpha = 0.135$ and $\Phi = 0.1$, whereas the dashed curve is obtained from Eq. (10) with $C_S = 2$. The agreement is fair for the yield stress but we still have a critical deformation which is lower in the microscopic model. In this figure we have also shown the result predicted by Rosensweig where the stress is taken from the torque on the structure. We can see (dash-dotted line) that this approach overestimates the critical strain (which is obtained for $\theta = 45°$ or $\gamma = 1$) and underestimates the yield stress. We have checked that the dependence of the yield stress on the volume fraction was also fairly represented by Eq. (10) for the slab structure.

At this stage we could conclude that Eq. (10) is able to describe quantitatively the dependence of the yield stress on the volume fraction for different structures. This is still to be verified for high values of the control parameter α.

B. Test of the macroscopic approach for $\alpha \gg 1$

For high values of α, the short range interactions between particles become more and more important and we do not expect that a global macroscopic approach based on shape

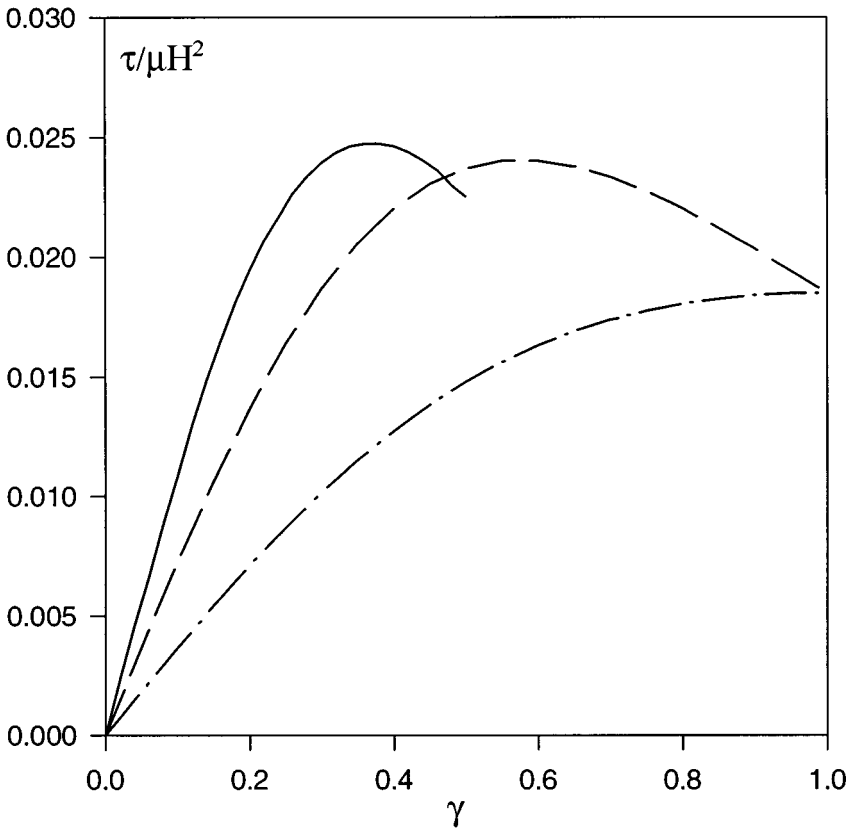

FIG. 6. Normalized stress vs strain. Comparison between microscopic and continuum models for stripes with $\alpha = 0.135$ and an average volume fraction $\Phi = 0.1$. —— Microscopic model, — — — Macroscopic model [Eq. (10) with $C_s = 1$], - — - Macroscopic model from Rosensveig (1995).

anisotropy of aggregates could be able to represent the evolution of the yield stress with the volume fraction. This is well illustrated in Fig. 7 where we compare for $\alpha = 50$ the normalized yield stress for a cubic array of chains of spheres with the macroscopic approach based on cylinders. Whereas the microscopic derivation (dots) gives a stress which increases linearly with the volume fraction, we obtain, with the macroscopic approach, values which are far too small and furthermore which saturate with the volume fraction (squares). Nevertheless, it is interesting to note that if we take only into account the dipoles in the microscopic derivation, then the prediction (triangles) is very close to the values obtained by the macroscopic approach. This is consistent with the fact that dipolar interactions are long ranged and not sensitive to the small changes of distance between the surfaces of the particles. The importance of short range multipolar interactions for the calculation of the yield stress when $\alpha \gg 1$ is well known but what we want to emphasize here is the role played by the rupture of contacts between particles, compared to the role played by the shape anisotropy of aggregates. In order to understand this point we have compared the yield stress obtained for a slab structure where the stripes are formed of single planes of spheres with inside each plane a cubic packing. These stripes can be strained either parallel or perpendicularly to their own plane. We have plotted the microscopic model predictions for $\Phi = 0.2$ and $\alpha = 38$ in Fig. 8. We can see that the

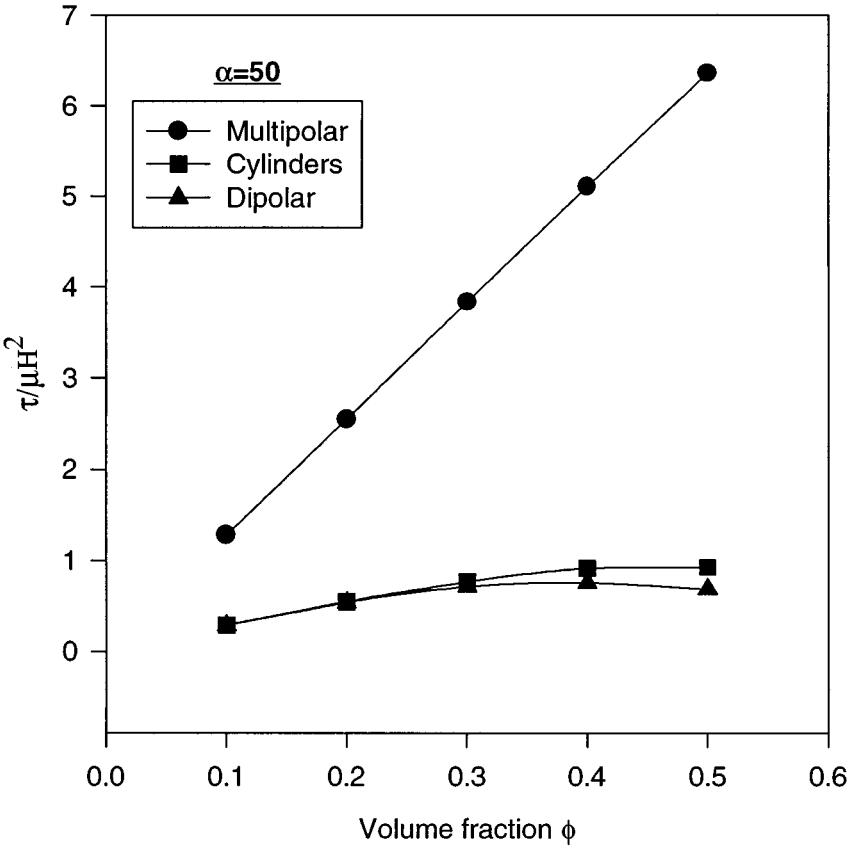

FIG. 7. Normalized yield stress vs volume fraction for $\alpha = 50$. (●●●) Full microscopic model for cubic lattices of chains. (▲▲▲) Microscopic model with only dipolar interactions. (■■■) Macroscopic model for cylindrical aggregates.

difference of behavior between the two directions of shear is quite negligible; similar results are found with $\phi = 0.5$ and $\alpha = 38$ where the yield stresses are, respectively, $\tau_{\parallel}^{y}/\mu H^2 = 4.77$ and $\tau_{\perp}^{y}/\mu H^2 = 4.84$ with the same critical strain $\gamma_c = 0.08$. In opposition the macroscopic model would give zero stresses for the direction of strain parallel to the stripes since, from a macroscopic point of view, the shape of a stripe of infinite length does not change if it is sheared in its own plane. It is then clear that a macroscopic model is completely unable to predict the yield stress at high values of α.

Actually for high values of α, not only do we need to use the microscopic derivation with a multipolar development, but we also need to know how the ruptures will occur during the strain of the aggregates. To illustrate this last point let us consider two structures with the same average volume fraction $\phi = 0.2$. The first one is made of individual monolayers of simple cubic array of spheres (structure P1), and the second one is made of distorted planes of particles (P1d, Fig. 3): each column in the y-z plane is made in such a way that it can be strained without the need to break a contact between two particles, at least as long as the strain is less than $\gamma_c = \sqrt{(16a^2/h^2)-1}$, which corresponds to the complete extension of the column. The yield stress calculated for these two structures with the same values of α and Φ is dramatically different as can be seen by

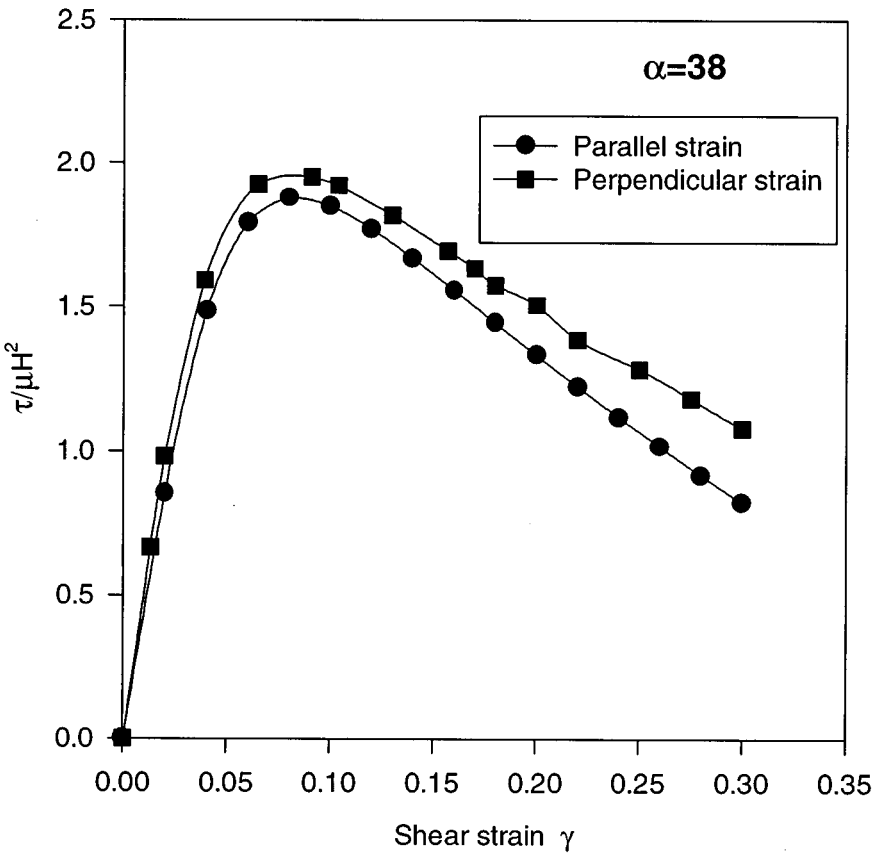

FIG. 8. Microscopic model for the normalized yield stress of a layered structure formed of simple cubic planes with $\alpha = 38$ and $\Phi = 0.2$. (●●●) Strain parallel to the orientation of stripes. (■■■) Strain perpendicular to the orientation of stripes.

comparing Figs. 8 and 9. In the standard model the separation of the particles occurs from the beginning but the tangential magnetic force grows proportionally to $\sin\theta \propto \gamma$, so the maximum of the tangential force does not occur when the separation of spheres begins but at higher strain (cf. Fig. 8). On the contrary in the second structural model the force on the structure remains low as long as the particles slide on each other and remain in contact. When all the spheres become aligned, (at $\gamma = 0.808$ in our particular case with $h = 28/9$) the chain has to be broken and the component of the magnetic force which opposes the straining force is proportional to $\cos^2\theta \sin\theta$. This is why we have this large jump in the stress needed to break the structure. The yield stress shown by the arrow in Fig. 10 requires a careful calculation of the change of energy above the breaking strain in order to get good accuracy on its derivative which is the yield stress. We see that its value is seven times larger than in the standard model (Fig. 8) for the same density and the same α. Of course this zig-zag structure P1d is quite arbitrary but it allows one to understand the importance of the angle between the direction of the field and the line of centers of a pair of particles which are separating. Actually we expect that, in real

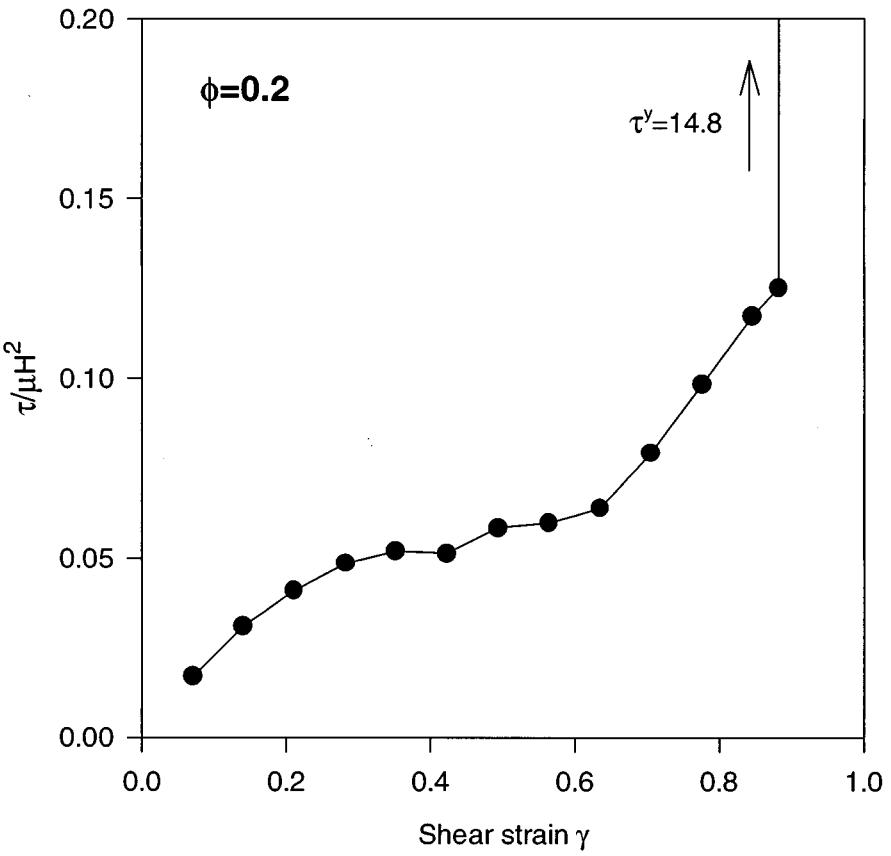

FIG. 9. Normalized yield stress for the structure P1d shown in Fig. 3. The jump corresponds to the rupture of the chains.

aggregates, the ruptures between pairs of particles can occur at any angle between zero and a critical angle of about 45° and not only at the low angles predicted by the standard model.

The same kind of behavior can be obtained more simply by studying the force on a pair of spheres. This force can be written (Klingenberg 1990)

$$\mathbf{f} = \left(\frac{a}{r}\right)^4 [(2 f_{\parallel} - f_{\perp}) \cos^2 \theta \, \mathbf{e}_r + f_{\Gamma} \sin 2\theta \mathbf{e}_{\theta}], \tag{12}$$

where $f_{\parallel}$, $f_{\perp}$, and f_{Γ} are functions of the separation between the two spheres and of the permeability ratio α. These functions are calculated by a multipolar development; they are equal to unity in the dipolar approximation.

If the pair of particles is rotating, the spheres remain in contact and the radial force coming from the field is equilibrated by the mechanical contact force, so it is only the x component of the tangential force on the pair of particle which will resist the strain, that is to say:

$$f_x = \left(\frac{a}{r}\right)^4 f_{\Gamma} \sin 2\theta \cos \theta \quad \text{for} \quad \gamma < \gamma_c. \tag{13}$$

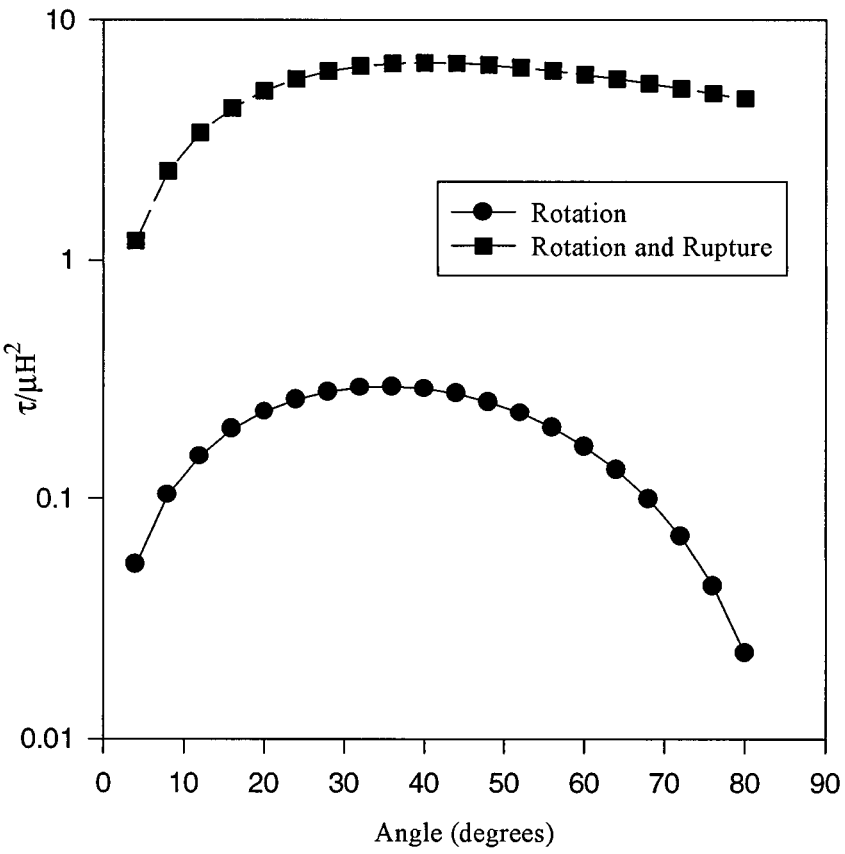

FIG. 10. Jump of stress vs the angle where the rupture of the contact between the two spheres occurs. (●●●) Yield stress associated to the torque on a pair of spheres. (■■■) Yield stress associated with the rupture after a rotation of a given angle.

If we assume that for $\gamma > \gamma_c$ the particles will separate, then the mechanical contact force disappears and we recover the parallel component of the force. Actually, when $\alpha \gg 1$ the function $f_{\parallel}$ is much larger than $f_{\perp}$ or f_{Γ} so we can write for the tangential force f_x:

$$f_x = \left(\frac{a}{r}\right)^4 2\, f_{\parallel} \sin\theta \cos^2\theta \quad \text{for} \quad \gamma > \gamma_c . \tag{14}$$

The difference in the values of $f_{\parallel}$ and $f_{\perp}$ or f_{Γ} explains the discontinuity which is observed in Fig. 9. Of course, in effect the yield stress will be limited by the saturation of the magnetization for MR fluids or by dielectric breakdown or conductivity effects for ER fluids. Furthermore due to averaging on different microscopic structures, a stress-strain curve as the one represented in Fig. 9 is not observed in usual MR or ER fluids. Nevertheless, it is possible to observe it on a model of MR fluid based on chains of steel spheres. In Fig. 10 we show the stress calculated from the tangential force on a rotating pair of spheres [cf. Eq. (13)] for a volume fraction $\Phi = 0.2$ assuming that the force on a couple of spheres is representative for the restoring force on a chain (dots). On the same graph (solid squares) we have plotted the yield stress [obtained from the x component of

TABLE I. Yield stress (π/μ H^2) with $\alpha = 38$ for different structures and different modes of rupture: C1—Lattice of simple chains with a square basis, affine trajectories; C2S—Lattice of shifted double chains with a square basis, nonaffine trajectories; P2—Simple cubic planes with a width of 2 particles (4a), affine trajectories; P4—Simple cubic planes with a width of 4 particles (8a), affine trajectories; P2S—Planes made with shifted double chains [width $(2+\sqrt{3})$a], affine trajectories; P1d—Planes made with distorted simple chains, nonaffine trajectories; C2S′—Same lattice as C2S but with affine trajectories.

Structure	C1	C2S	P2	P4	P2s	P1d	C2S′
$\phi = 0.2$	1.92	1.90	1.96	1.90	1.85	14.8	5.43
$\phi = 0.4$	3.79		3.87	3.80	3.66		

the force in Eq. (12)] corresponding to the separation of a pair of spheres after they have rotated up to the angle $\theta = \text{arc tg}(\gamma)$. The difference between the two curves for a given angle corresponds to the jump of stress due to the separation of the two spheres after the period of rotation. Of course this two sphere model only reproduces, semiquantitatively the more realistic structure we have discussed above, but it helps to predict the order of magnitude of this jump as a function of the strain.

We have done several calculations of the stress-strain relation for different values of α and different structures. Some of these results are presented in Table I for the normalized yield stress corresponding to $\alpha = 38$ and two values of the volume fraction: $\Phi = 0.2$ and $\Phi = 0.4$. The missing values for $\Phi = 0.4$, correspond to structures where the spheres would overlap at this density; the accuracy of the values given in this table is better than 1% and corresponds to the use of 30 to 40 multipolar orders. There are two things which are worth noting: first, the value of the yield stress depends only slightly on the structure and second it grows proportionally to the volume fraction; But these features are only true because in these structures, the rupture of the contacts occurs between pairs of particles whose line of centers is in the direction of the applied field. The two last columns correspond to the other situation where the rupture also occurs between pairs of particles whose line of center is not aligned with the electric field. For the structure P1d, this is the situation described previously where the rupture occurs at $\gamma = 0.808$ for an initial distance $h = 28/9$. The last column corresponds to another situation with double chains (C2S′, Fig. 3) where the particles are supposed to move along the velocity lines; then the rupture, instead of occurring only between pairs of particles aligned with the field (as in C2S), also occurs between the particles whose line of center makes an angle of 60° with the direction of the field. We still note the large increase in yield stress compared to the classical mode of rupture of C2S where all the ruptures between pairs occur at a low angle. Such a scenario of rupture has already been studied (Gulley and Tao, 1993) but in a dipolar approximation which did not allow to see this kind of effect. The rupture of links which are not aligned with the field will not happen if other possibilities of motion exist as in C2S but it can be the only way to strain the structure in more compact aggregates. It appears than the condition of the rupture of contacts between particles is quite important to determine the yield stress. In the absence of a model giving this information about the rate of rupture of pairs of particles as well as their orientation relatively to the field it is still quite difficult to predict the yield stress for $\alpha \gg 1$.

IV. CONCLUSION

The comparison of the macroscopic and microscopic approaches has shown that a macroscopic approach based on the anisotropy of shape of the aggregates is only valid for low values of α. The analytic equation [Eq. (10)] can be used to model the yield stress of

systems based on nonmagnetic particles in a ferrofluid. It predicts a maximum of the yield stress with the volume fraction and also that a layered structure would give a yield stress approximately two times larger than a structure based on cylindrical or ellipsoidal aggregates.

For high values of α this macroscopic approach represents quite well the results we can obtain from the microscopic approach in a dipolar approximation. When the value of α is high, it is well known that the multipolar approach is necessary, but we have emphasized in this work that the rupture of contacts between pairs of particles and, above all, the orientation of the line of centers of these particles relatively to the field are the main quantities which will determine the value of the yield stress. The yield stress predicted for ruptures occurring at strains of order one can be an order of magnitude larger than the one predicted by the standard model where the rupture takes place at very low strain. The elaboration of a model which could take into account the dynamics of the deformation and rupture of aggregates in a shear is beyond the scope of this article but it should be possible along these lines to have a correct description of the rheology of ER and MR fluids.

ACKNOWLEDGMENT

Computer time was provided by the IDRIS Center in France.

APPENDIX: DERIVATION OF THE YIELD STRESS FOR STRIPES AND CYLINDERS

We start from the general relation Eq. (4) with the magnetization $M_z = m_z/V = \mu_0 \chi_{zz} H$, where $H = H_0/(1+\chi_{zz})$ is the average field inside the suspension and χ_{zz} is the component of the average susceptibility tensor on the axis of the external field. Then, taking the derivative relatively to the strain we obtain:

$$\tau = \frac{1}{2} \mu_0 H^2 \frac{\partial \chi_{zz}}{\partial \gamma}, \tag{A1}$$

with

$$\chi_{zz} = \chi_{\parallel} \cos^2 \theta + \chi_{\perp} \sin^2 \theta. \tag{A2}$$

Due to the continuity of the tangential field we have, either for stripes or for cylinders:

$$\chi_{\parallel} = \Phi_s \chi_s + (1-\Phi_s)\chi_f. \tag{A3}$$

In Eq. (A3) the volume fraction Φ_s represents the part of the space occupied by the aggregates. This should not be confused with the internal volume fraction of the aggregates: Φ_a (we have: $\Phi_s = \Phi/\Phi_a$).

For a slab structure, the perpendicular component $\chi_{\perp}$ is obtained in the same way as the capacity of a layered composite structure:

$$\frac{1}{1+\chi_{\perp}} = \frac{\Phi_s}{1+\chi_s} + \frac{1-\Phi_s}{1+\chi_f} \text{ or } \mu_{\perp}^* = \frac{\mu_s^* \Phi_s}{1+\mu_s^*(1-\Phi_s)}. \tag{A4}$$

In the case of cylinders we neglect end effects and replace them by an assembly of disks with two dimensional electrostatics. In this case the 2D Maxwell Garnet theory gives:

$$\frac{\frac{\mu_\perp}{\mu_f}-1}{\frac{\mu_\perp}{\mu_f}+1}=\Phi_s\frac{\frac{\mu_s}{\mu_f}-1}{\frac{\mu_s}{\mu_f}+1} \text{ or } \mu_\perp^*=\frac{2\mu_s^*\Phi_s}{2+\mu_s^*(1-\Phi_s)}, \quad \text{with } \mu_\perp^*=\frac{\mu_\perp}{\mu_f}-1. \tag{A5}$$

Taking into account that $\mathrm{tg}(\theta) = \gamma$ we have the stress from A1 to A3 with the use of A4 for the slab structure and of A5 for the structure based on cylinders.

References

Bossis, G., Y. Grasselli, E. Lemaire, J. Persello, and L. Petit, ''Phase separation and flow induced anisotropy in electrorheological fluids,'' Europhys. Lett. **25**, 335–340 (1994).

Cebers, A., ''Transformation of concentration domain structures of liquid magnetic in plane layers 1. Energetical approach,'' Magnitnaya Gidrodinamika **31**, 61–68 (1995) (in Russian).

Chen, Y., A. F. Sprecher, and H. Conrad, ''Electrostatic particle-particle interactions in electrorheological fluids,'' J. Appl. Phys. **70**, 6796–6803 (1991).

Clercx, H. J. H., and G. Bossis, ''Many body electrostatic interactions in electrorheological fluids,'' Phys. Rev. E **48**, 2721–2738 (1993).

Clercx, H. J. H., and G. Bossis, ''Static yield stresses and shear moduli in electrorheological fluids,'' J. Chem. Phys. **103**, 9426–9437 (1995).

Davis, L. C., ''Polarization forces and conductivity effects in electrorheological fluids,'' J. Appl. Phys. **72**, 1334–1340 (1992).

Ginder, J. M., L. C. Davis, and L. D. Elie, ''Rheology of magnetorheological fluids: models and measurements,'' *Proceedings of the 5th Conf. on ER fluids and MR suspensions*, edited by W. A. Bullough (World Scientific, Singapore, 1996).

Grasselli, Y., G. Bossis, and E. Lemaire, ''Structure induced in suspensions by a magnetic field,'' J. Phys. II France **4**, 253–263 (1994).

Gulley, G. L., and R. Tao, ''Static shear stress of electrorheological fluids,'' Phys. Rev. E **48**, 2744–2751 (1993).

Halsey, T. C., J. E. Martin, and D. Adolf, ''Rheology of electrorheological fluids,'' Phys. Rev. Lett. **68**, 1519–1522 (1992).

Havelka, K., ''Novel material for electrorheological fluids,'' Polymer Reprints **35**, 315–316 (1994).

Klingenberg, D. J., and C. F. Zukoski, ''Studies on the steady shear behavior of electrorheological suspensions,'' Langmuir **6**, 15–24 (1990).

Landau, L. D., and E. M. Lifschitz, *Electrodynamics of Continuous Media*, 2nd ed. (Pergamon, New York, Vol. 8, 1984), pp. 41 and 116.

Lemaire, E., G. Bossis, and O. Volkova, ''Deformation and rupture mechanisms of ER and MR fluids,'' Int. J. Mod. Phys B **10**, 3173–3180 (1996).

Liu, J., T. Mon, G. A. Flores, J. Bibette, and J. Richard, ''The evolution of field induced structure of confined ferrofluid emulsions,'' *Proceedings of the Fourth International Conference on ER Fluids and MR Suspensions*, edited by R. Tao and G. B. Roy (World Scientific, Singapore, 1994), pp. 190–201.

Maxwell-Garnet, J. C., ''Colour in metal glasses and metallic films,'' Philos. Trans. R. Soc. London **203**, 385–391 (1904); **205**, 237 (1906).

Rosensweig, R. E., ''On magnetorheology and electrorheology as states of unsymmetric stress,'' J. Rheol. **39**, 179–192 (1995).

Shulman, Z. P., V. I. Kordonsky, E. A. Zaltsgendler, I. V. Prokhorov, B. M. Khusid, and S. A. Demchuk, ''Structure, physical properties and dynamics of magnetorheological suspensions,'' Int. J. Multiphase Flow **12**, 935–955 (1986).

Volkova, O., G. Bossis, E. Lemaire, V. Basktovoi, and Matoussevitch, ''Magnetorheology in strongly structured media,'' Magnitnaya Gidrodinamika **4**, 304–310 (1996).

Weiss, K. D. and T. G. Duclos, ''Controllable fluids: the temperature dependence of post-yield properties,'' *Proceedings of the Fourth International Conference on ER fluids*, edited by R. Tao and G. D. Roy (World Scientific, Singapore, 1994), pp. 43–59.